

平成 25年度三重大学大学院生物資源学研究科修士論文

**Influence of Regional Cold Okhotsk SST upon
Remote Atmospheric Circulation in Summer**

夏季オホーツク海の局所的な低水温が

もたらす大気場への遠隔影響

*Climate and Ecosystems Dynamics Division Graduate school of Bioresources Mie
University*

512M233 Satoshi Fujita *Supervisor:* Prof. Yoshihiro Tachibana

February 26, 2014

Abstract

Okhotsk Sea, it is a sea area has been a "sea of mystery" from the lack of observational data.

Okhotsk Sea is the north of Japan; Okhotsk high that occurs in summer is heavily involved in cool summer and Baiu season in Japan. To correctly evaluate the influence of Okhotsk high is essential to weather forecast of Japan. However, as mentioned, Okhotsk Sea is a "sea of mystery" from the lack of observational data, the detailed mechanism of Okhotsk high has not yet been clear. In this study, using the radiosonde data in Okhotsk Sea, which was observed in 2006 and 1998, and the calculation results of regional climate model in close vertical resolution, to clarify how the low sea surface temperature (SST) in Okhotsk Sea affects the synoptic scale disturbance and the atmospheric boundary layer. SST used as boundary conditions in the model is higher than SST observed in Bussol Sea, where is known SST is very low. To estimate the effect of low SST gives the atmosphere in Bussol Sea around, providing a run with a lower 5K boundary conditions of the SST (COLD), which is compared with a normal run (CTL). From the observation, large surface inversion layer is observed in Bussol Sea. Surface inversion layer is reproduced in the COLD run. However it is not reproduced in the CTL. It is clear that this surface inversion is formed by low SST around Bussol Sea. In comparing the COLD run and CTL run, high pressure deviation in SST decrease area and low pressure deviation in the southwest are formed in COLD run. The conditions to be formed this low pressure deviation is that high pressure is the north and low pressure is the south across the Kuril Islands, and northeast wind blow on SST decrease area. It is considered wave of pressure associated with baroclinic instability wave has propagated and low pressure deviation is formed. The results of this study suggest that low SST of Bussol Sea affects remotely.

Contents

1. Introduction.....	4
2. Data and method.....	6
3. Result.....	9
3.1. Vertical structure of temperature.....	9
3.2. Calculation results of the model.....	9
3.2.1 Verification of reproducibility	9
3.2.2 Time series cross section.....	10
3.2.3 Synoptic scale disturbance.....	11
4. Discussion.....	12
Acknowledgment.....	14
References.....	15
Figure captions.....	19

1. Introduction

It has been common that middle-latitude small-scale anomalous sea surface temperature (SST) locally influences atmospheric circulations just over the anomalous SST area, in particular in the Kuroshio and Gulf Stream regions [e.g., Sweet et al., 1981; Minobe et al., 2008; Tanimoto et al., 2009]. However, it has not been common that middle-latitude small-scale anomalous SST can remotely influence atmospheric circulations far from the anomalous SST area. This study demonstrates that a small-scale cold SST spot located between the North Pacific Ocean and the Okhotsk Sea remotely influences synoptic-scale circulations.

The Okhotsk Sea (Figure 1) is semi-enclosed by Sakhalin Island, mainland Russia, and the Kamchatka Peninsula, and the Kuril Islands separate it from the Pacific Ocean. The Okhotsk Sea has two extraordinary climatic characteristics. One is the sea ice formation. Very cold air outbreak from Siberia in winter enables the Okhotsk Sea to be covered by sea ice in the southernmost area in Northern Hemisphere. The sea ice remaining until June keeps the SST cold in summer. The other is strong tidal mixing. In the Okhotsk Sea region a strong tidal flow combined with strong vertical mixing causes cold intermediate water to crop out around the Kuril Islands [Nakamura et al., 2000a, b]. As a result, spots with very cold SST form there. The intermediate cold water formation is related mainly to the wintertime sea ice formation in the Okhotsk Sea [Talley, 1991; Ohshima et al., 2002; Shcherbina et al., 2003]. Summertime SST in the Okhotsk Sea cold spots as low as 5 °C have been reported [e.g., Tachibana et al., 2008; Tokinaga and Xie, 2009]. These two extraordinary climatic characteristics make the SST lower than any other SSTs in other Northern Hemisphere seas at the same latitude. An anticyclone covering the cold Okhotsk Sea, referred to as Okhotsk high, is occasionally formed with cold marine-boundary layer associated with fog and low-level cloud between latter April and early September. [Nakamura and Fukamachi 2004; Tachibana et al., 2004;

Tachibana et al., 2008]. The southward advection of the cold boundary-layer air mass associated with the Okhotsk high brings about cool summer in Japan [Kodama, 1997; Ninomiya and Mizuno, 1985; Nakamura and Fukamachi 2004] (Figure 2).

Some numerical simulations showed that the Okhotsk cold SST can raise the local sea level pressure [Tokinaga and Xie, 2009; Koseki et al, 2012]. Koseki et al. (2012) showed that the formation of low-level clouds associated with the cold SST strengthens the Okhotsk high by a regional climate model. A numerical model by Tokinaga and Xie (2009) demonstrated that the small-scale cold SST spot formed by the ocean tidal mixing over the Kuril Islands is able to raise the overlying sea level pressure (SLP) locally. Although these numerical approaches successfully captured the local SLP rise over the cold SST, the comparison of simulated atmospheric structures over the cold SST spot with direct upper air observations by radiosondes is crucial. We need to assess the reproducibility of numerical simulations by direct upper air observations in the Okhotsk Sea. However, radiosonde observations over the Okhotsk Sea, in particular over the cold spot, are few. Only twice of the upper-air field campaign are executed in 1998 and 2006 [Tachibana et al., 2008]. Tachibana et al. (2008) showed that extremely cold air-mass in the marine-boundary layer associated with dense fog or low-level cloud over the Okhotsk Sea frequently observed. This observational result suggests that such fog or low-level cloud as in Tachibana et al. (2008) must be reproduced in a numerical model study. Vertically high resolution numerical model may simulate fog or low-level cloud. The first purpose of the present study is to show that influence of the local small-scale cold SST spot along the Kuril Islands upon an enhancement local anticyclone by a numerical model with high vertical resolution in the lower troposphere in comparison with the radiosonde data reported by Tachibana et al., (2008).

As mentioned above, the southward advection of the cold boundary-layer air mass brings about cool summer in Japan. If a cyclonic circulation is located to the south

of the Okhotsk high, it is efficient for the southward advection of the Okhotsk cold air mass. Kodama et al. (2009) showed that cold marine boundary air masses off eastern coast of Japan occasionally come from the Okhotsk Sea by a trajectory analysis (Figure. 4 and Figure. 15 in Kodama et al (2009)). Tachibana et al. (2004) showed that a cyclonic circulation tends to occur to the south of the Okhotsk high. These previous results suggest that the presence of a pair of the northern Okhotsk high and the southern low is important to make Japan cool. The second purpose of the present study is to show that the southern low is strengthened by a remote influence of the cold SST spot along the Kuril Islands by a numerical simulation and statistical data analysis.

2. Data and model simulation

This study uses GPS radiosondes data taken by Russian research vessel Khromov [Tachibana et al., 2008]. In 1998 observation, GPS radiosondes were launched over the Okhotsk Sea four times daily (0000, 0600, 1200, and 1800 UTC) from 9 July through 18 July and twice daily (0000 and 0012 UTC) from 19 July through 25 July (Figure 3). In 2006 observation, GPS radiosondes were launched four times daily (0000, 0600, 1200, and 1800 UTC) from 16 August through 31 August (Figure 4). For each observation, surface atmospheric and oceanic measurements were executed four times daily with inclusion of sea level pressure (SLP), SST, surface air temperature (SAT), surface wind, surface humidity, and cloud cover. The Japanese 25 Year Reanalysis (JRA25) 6 hours data with horizontal resolution $1.25^{\circ} \times 1.25^{\circ}$ from 1979 to 2004, and Japan Meteorological Agency Climate Data Assimilation System (JCDAS) data from 2005 to 2010 are also used in this study [Onogi et al., 2007].

The International Pacific Research Center, University of Hawaii, regional climate model (IPRC-RegCM, now referred to as iRAM) [Wang et al., 2003] is used in this study in order to designate to the experiment to determine influence of the cold SST area along the Kuril Islands upon the atmospheric circulation. This model is succeeded in the reproduction of low-level clouds over the Okhotsk Sea [(Koseki et al., 2012)]. The horizontal resolution is $0.25^{\circ} \times 0.25^{\circ}$. The number of vertical levels is 36, and σ as the vertical coordinate; top level pressure is 100 hPa. We made vertical resolution of the lower troposphere high; 20 levels below 0.7σ . Atmosphere scheme adopted in this study is the same as Koseki et al. (2012); Physical parameterizations for radiation [Edwards and Slingo, 1996; Chou et al. 1998], cumulus convection [Tiedtke, 1989; Nordeng, 1995], turbulence vertical mixing [Detering and Etling, 1985], and cloud microphysics [Wang, 2001]. The cloud microphysics consists of six hydrometeors: rain, cloud liquid water, cloud ice, snow, graupel, and water vapor. Land surface scheme is that

Biosphere-Atmosphere Transfer Scheme (BATS) [Dickinson et al., 1993]. For More details, we refer to Wang (2001) and Wang et al. (2003, 2004, 2007).

The model domain is set to be $35^{\circ}\text{N} - 65^{\circ}\text{N}$ and $130^{\circ}\text{E} - 170^{\circ}\text{E}$. The lateral boundary condition is set using 6 hourly JRA25/JCDAS data: zonal wind, meridional wind, temperature, specific humidity, and cloud liquid water. These lateral boundary conditions are linearly interpolated in time at every time step. Over the ocean, we use National Oceanic and Atmospheric Administration (NOAA) optimum interpolation sea surface temperature (OISST, daily), with an original resolution of $0.25^{\circ} \times 0.25^{\circ}$, as lower boundary condition.

The comparison of the OISST with direct measurement the SST is shown in Figure. 5. Obviously, the observed SST near the Kuril Island was much lower than OISST. Thus, we use two kinds of boundary conditions. One is the same surface boundary condition as the OISST, which is referred to control run (CTL). The other is that SST near the Kuril Islands is set as 5 K lower than the OISST, which is referred as cold SST spot run (COLD). Because Nakamura et al (2000a, b) pointed that the areas along the Kuril Islands have large tidal mixing with outcrop of cold intermediate water, the area along the Kuril Islands must be set colder than other areas in the COLD run. The area that we decreased SSTs by 5 K is $150^{\circ}\text{E} - 152.5^{\circ}\text{E}$ and $45^{\circ}\text{N} - 48^{\circ}\text{N}$, $152.5^{\circ}\text{E} - 155^{\circ}\text{E}$ and $46.5^{\circ}\text{N} - 49.5^{\circ}\text{N}$, and $155^{\circ}\text{E} - 157.5^{\circ}\text{E}$ and $48^{\circ}\text{N} - 51^{\circ}\text{N}$ (Figure 6). COLD run, which includes the influence of ocean tidal mixing, is regarded as the real run, whereas CTL run is regarded as the one without the influence of the tidal mixing.

3. Results

3.1. Vertical structure of temperature

In 1998 and 2006, 16 and 20 radiosondes were respectively launched in the Bussol Strait, in which the tidal mixing is strong. For each point, we calculate vertically averaged temperature from surface to 3000m, and subtract the average temperature from observed temperature (Figure 7). All the 36 points over Bussol Sea have sharp inversion layer from the surface to about 500m high. Large-scale weather conditions in an observational year are different from the other, and also they changed day by day during each observation period. Nevertheless, vertical temperature profile did not largely change. The wind direction and its speed, and mixing ratio in 1998 and 2006 were clearly different between each other, and they changed day-by day (Figure not shown). Thus, we consider that the temperature in the lower troposphere is consistently forced by cooling from sea surface regardless of large-scale weather conditions. Over the inversion layer, very dry mixed layer is observed in the profile of the most on the top of inversion layer.

3.2. Calculation results of the model

3.2.1 Verification of reproducibility

Using the model grid points closest to the 37 observation point on the Bussol Strait, we execute similar analysis to the observation. In order to verify the model reproducibility (Figure 8). Even in 1998 and 2006, the CTL run failed to simulate the surface strong inversion layer such as in the observations. In COLD run such surface inversion layer as in the observations are clearly seen. The average temperature in July 1998 in the COLD run is lower than CTL run over 100m (about 0.989σ). However, up to 1200m (about 0.876σ) from 300m (about 0.967σ), COLD run is warmer than CTL. The mixing ratio in CTL run is generally consistent with the observed value, however

COLD run simulates the mixing ratio more consistently with the observation (Figure not shown). Both runs do not capture the change in fine wind speed and wind direction like observations. Still, it is sufficient to see the changes in the wind of synoptic scale. From these comparisons, we can confirm that COLD run is regarded as a reproducible run, whereas the CTL run as the one without the influence of the oceanic tidal mixing.

3.2.2 Time series cross section

We note that the difference between the temperature of the COLD run and CTL run is large in July 1998. In order to see the time evolution of temperature, the area-averaged temperature profile of the SST decrease area we create time series of cross section from July 1, 1998 until July 31, 1998 (Figure 9). Temperature rises to the border July 15. Research ship Khromov has had observed Bussol Sea is a 15 to 18, it has been observed period high temperature just right.

To compare the CTL and COLD run, over the entire period, temperature of up to 100m sea level of COLD run is as low as about 3 K than CTL. This is due to the difference of the sensible heat flux from the sea surface. The 11 to 14, low temperature deviation occurs up to an altitude of 500m. The 15 to 18, in 1200m altitude 300m temperature of COLD run is high about 2 K than CTL. At this period, temperature rises due to reduced SST. Similarly, we compare long wave radiation, short wave radiation, large scale condensation, vertical mixing, sum of the four variables (sum of heat) (Figure 10 top), vertical flow (Figure 10 bottom), and cloud cover in the CTL and COLD run. Sum of heat is defined as degC/day, vertical flow is omega, and cloud cover is represented by 0-1. In the entire period, cooling in COLD run near sea level is strong. The 11 to 14, negative deviation of sum of heat occurs up to an altitude of 500m, and at the same position cloud cover is large. And in the sky, downward flow is enhanced.

3.2.3 Synoptic scale disturbance

We note July 11 to 14. In both CTL and COLD run, there is a high pressure to the north and a low pressure to the south across the Kuril Islands; northeast wind blows (Figure 11 and 12). In SST decrease area, for COLD run low level cloud is more than CTL (Figure 13). The low level cloud referred to here is the average cloud cover from $\sigma = 0.982$ (about altitude 150m) to $\sigma = 0.942$ (about altitude 500m). For COLD run pressure is higher than CTL in SST decrease area. And low pressure deviation is formed in the southwest of this high pressure deviation (Figure 14).

4. Discussion

Low level clouds for COLD run is more than CTL from 11 to 14. Therefore, strong cooling occurs in the lower layer by the long wave radiation. It is considered the downward flow is enhanced by the upper layer in order to compensate for cooling, to form a cold high pressure deviation with the lower clouds. There is a high pressure to the north and a low pressure to the south across the Kuril Islands, and northeast wind blows. For the northeast wind, cold air on SST decrease area moves on the warm sea in south. Cold air is heated by the sensible heat flux and upward flow is enhanced. In addition, the north area of northeast wind is cold in order to lower the SST, and the south has a high temperature. Therefore, temperature gradient becomes steep, and generation of low pressure due to baroclinic instability is suggested along this northeast wind. It is considered wave train of high and low pressure is seen along the northeast wind, wave of pressure associated with baroclinic instability wave has propagated.

It is important for this mechanism that the northeast wind blows in Bussol Sea. For geostrophic wind, it is condition of blowing northeast wind that there is a high pressure to the north and a low pressure to the south across the Kuril Islands. Therefore, using the calculation results of the July of 1990 to 2010 of CTL, the days that the difference between the area average pressure of $145^{\circ}\text{E} - 155^{\circ}\text{E}$, $48^{\circ}\text{N} - 54^{\circ}\text{N}$ and area average pressure of the same longitude $36^{\circ}\text{N} - 42^{\circ}\text{N}$ is or more 6.5hPa is picked up for composite analysis. In comparing the CTL and COLD run, northeast high pressure deviation and southwest low pressure deviation of Bussol is formed (Figure 15). This indicates that the local change of SST around Bussol Sea influences not only the atmosphere immediately above, widely downstream side. To form southwest low pressure deviation, northeast wind anomalies occur in the Tohoku region of Japan. The northeast wind corresponds to that wind affected by the cold sea to land in the Tohoku region. It is said northeast winds in the Tohoku region in the summer such as this is

called Yamase for a long time, to result in a poor harvest of rice and cold summer in the Tohoku region. The results of this study suggest that low sea surface temperature of Busool Sea affects Yamase remotely.

Acknowledgment

I express gratitude to Professor Tachibana, my supervisor. He taught me the basic knowledge of the physics and detailed knowledge of the physical oceanography and the atmospheric dynamics and amenity of Okhotsk Sea. Additionally, many professors of Geosystem Science, Graduate school of Bioresources, Mie University advised me. I thank that very much.

Tomohiro Nakamura of Institute of Low Temperature Science Hokkaido University and Shunya Koseki of Nanyang Technological University Singapore taught me the calculation of regional climate model and provided me computation environment. I thank Yusuke Utagawa of KOZOKEIKAKU ENGINEERING and Tokyo University provided me the Khromov radiosonde data in 1998. Wataru Ofuchi of JAMSTEC and Ryohei Suzuki of Tokyo Tech University provided me vertical one dimensional radiative convection model. I was helped by their advices. I express gratitude to them. Members of climate and ecosystems dynamics laboratory provided some advices for my research. In particular, I got a lot of assistance from the students of doctoral course. I would like to thank for them.

References

- Chou, M., M. J. Suarez, C. H. Ho, M. M. H. Yan, and K. T. Lee (1998), Parameterizations for cloud overlapping and shortwave single-scattering properties for use in general circulation and cloud ensemble models. *J. Climate*, **11**, 202–214.
- Detering, H. W., and D. Etling (1985), Application of the E- ϵ turbulence model to the atmospheric boundary layer. *Bound.-Layer Meteor.*, **33**, 113–133.
- Dickinson, R. E., A. Henderson-Sellers, and P. J. Kennedy (1993), Biosphere–atmosphere transfer scheme (BATS) version 1 as coupled to the NCAR Community Climate Model. *Tech. Note NCAR/TN-387 + STR*, 72 pp., National Center for Atmospheric Research, Boulder, Colo.
- Edwards, J. M., and A. Slingo (1996), Studies with a flexible new radiation code. I: Choosing a configuration for a large-scale model. *Quart. J. Roy. Meteor. Soc.*, **122**, 689–719.
- Kodama, Y. M. (1997), Airmass transformation of the Yamase Air-flow in the summer of 1993, *J. Meteorol. Soc. Jpn.*, **75**, 737–751.
- Kodama, Y. M., Y. Tomiya and S. Asano (2009), Air mass transformation along trajectories of airflow and its relation to vertical structures of the maritime atmosphere and clouds in Yamase events. *J. Meteorol. Soc. Jpn.*, **87**, 665–685
- Koseki, S., T. Nakamura, H. Mitsudera, and Y. Wang (2012), Modeling low-level clouds over the Okhotsk Sea in summer: Cloud formation and its effects on the Okhotsk high. *J. Geophys. Res.*, **177**, D05208, doi:10.1029/2011JD016462, in press.

- Minobe, S., A. Kuwano Yoshida, N. Komori, S. P. Xie, and R. J. Small (2008), Influence of the Gulf Stream on the troposphere. *Nature*, **452**, 206–209, doi:10.1038/nature06690.
- Nakamura, T., T. Awaji, T. Hatayama, K. Akitomo and T. Takizawa (2000a), Tidal exchange through the Kuril Straits. *J. Phys. Oceanogr.*, **30**, 1622–1644, doi: 10.1175/1520-0485(2000)030 <1622:TETTKS>2.0.CO;2.
- Nakamura, T., T. Awaji, T. Hatayama, K. Akitomo, T. Takizawa, T. Kono, Y. Kawasaki and M. Fukasawa (2000b), The Generation of Large-Amplitude Unsteady Lee Waves by Subinertial K1 Tidal Flow: A Possible Vertical Mixing Mechanism in the Kuril Straits. *J. Phys. Oceanogr.*, **30**, 1601–1621, doi: 10.1175/1520-0485(2000)030<1601:TGOLAU>2.0.CO;2.
- Nakamura, H., T. Fukamachi (2004), Evolution and dynamics of summertime blocking over the Far East and the associated surface Okhotsk high. *Q. J. R. Meteorol. Soc.*, **130**, 1213-1233
- Ninomiya, K. and H. Mizuno (1985), Anomalous cold spell in summer over northeastern Japan caused by northeasterly wind from polar maritime airmass. *J. Meteorol. Soc. Jpn.*, **63**, 845–871.
- Nordeng, T. E. (1995): Extended versions of the convective parameterization scheme at ECMWF and their impact on the mean and transient activity of the model in the Tropics. *Res. Dep. Tech. Memo.* **206**, 41 pp., ECMWF.
- Ohshima, K. I., M. Wakatsuchi, Y. Fukamachi, and G. Mizuta (2002), Near-surface circulation and tidal currents of the Okhotsk Sea observed with satellite-tracked drifters. *J. Geophys. Res.*, **107**, 3195, doi:10.1029/2001JC001005.
- Onogi, K. et al (2007), The JRA-25 reanalysis, *J. Meteorol. Soc. Japan*, **85**, 369–432.

- Shcherbina, A. Y., L. D. Talley, and D. L. Rudnick (2003), Direct observations of North Pacific ventilation: brine rejection in the Okhotsk Sea. *Science*, **302**, 1952–1955, doi: 10.1126/science.1088692.
- Sweet, W., R. Fett, J. Kerling, and P. La Violette (1981), Air-sea interaction effects in the lower troposphere across the north wall of the Gulf Stream. *Mon. Weather Rev.*, **109**, 1042–1052, doi:10.1175/1520-0493(1981)109<1042:ASIEIT>2.0.CO;2.
- Tachibana, Y., K. Iwamoto, and M. Ogi (2004), Abnormal meridional temperature gradient and its relation to the Okhotsk high. *J. Meteor. Soc. Japan.*, **86**, 753-771
- Tachibana, Y., K. Iwamoto, H. Ogawa, M. Shiohara, K. Takeuchi, and M. Wakatsuchi (2008), Observational study on atmospheric and oceanic boundary-layer structures accompanying the Okhotsk anticyclone under fog and non-fog conditions. *J. Meteorol. Soc. Jpn.*, **86**, 753–771.
- Talley, L.D. (1991), An Okhotsk Sea water anomaly: Implication for ventilation in the North Pacific. *Deep Sea Res. Part I*, **38**, 171–190.
- Tanimoto, Y., S. P. Xie, K. Kai, H. Okajima, H. Tokinaga, T. Murayama, M. Nonaka, and H. Nakamura (2009), Observations of marine atmospheric boundary layer transitions across the summer Kuroshio Extension. *J. Clim.*, **22**, 1360–1374, doi:10.1175/2008JCLI2420.1.
- Tiedtke, M. (1989), A comprehensive mass flux scheme for cumulus parameterization in large-scale models. *Mon. Wea. Rev.*, **117**, 1779–1800.
- Tokinaga, H., and S. P. Xie (2009), Ocean tidal cooling effect on summer sea fog over the Okhotsk Sea. *J. Geophys. Res.*, **114**, D14102, doi:10.1029/2008JD011477.

- Wang, Y. (2001), An explicit simulation of tropical cyclones with a triply nested movable mesh primitive equation model—TCM3. Part I: Model description and control experiment. *Mon. Wea. Rev.*, **129**, 1370–1394.
doi:10.1175/1520-0493(2001)129<1370:AESOTC>2.0.CO;2.
- Wang, Y., O. L. Sen, B. Wang (2003), A Highly Resolved Regional Climate Model (IPRC-RegCM) and Its Simulation of the 1998 Severe Precipitation Event over China. *J. Climate*, **16**, 1721–1738.
doi:10.1175/1520-0442(2003)016<1721:AHRRCM>2.0.CO;2
- Wang, Y., S. P. Xie, and H. Xu (2004a), Regional model simulations of marine boundary layer clouds over the southeast Pacific off South America. Part I: Control wxperiment. *Mon. Weather Rev.*, **132**, 274-296,
doi:10.1175/1520-0493(2004)132<0274:RMSOMB>2.0.CO;2
- Wang, Y., H. Xu and S. P. Xie (2004b), Regional model simulations of marine boundary layer clouds over the southeast Pacific off South America. Part II: Sensitivity experiments, *Mon. Weather Rev.*, **132**, 2650-2668,
doi:10.1175/MWR2812.1
- Wang, Y., L. Zhou, and K. Hamilton (2007), Effect of convective entrainment/detrainment on the simulation of the tropical precipitation diurnal cycle. *Mon. Weather Rev.*, **135**, 567-585, doi:10.1175/MWR3308.1.

Figure captions

Figure 1 Map of the Okhotsk Sea and Kuril Islands.

Figure 2 Surface weather chart based on the JRA25, showing unfiltered mean-sea-level pressure for 12 July 1998 (heavy solid lines at 2 hPa intervals), inferred surface air temperature anomalies (dashed lines and shaded at -3, -4, -5 degC).

Figure 3 The observation route of Khromov in 1998, showing observation point (blue dot) and observation number.

Figure 4 The observation route of Khromov in 2006, showing observation point (blue dot) and observation number.

Figure 5 SST observed by Khromov (red line) and SST based on NOAA OISST of the nearest grid from observation point (blue line). Top is in 1998, and bottom is in 2006.

Figure 6 SST based on NOAA OISST (daily) (shading 2 degC intervals) of SST decrease run in 17 July. Red frame area is SST decrease area.

Figure 7 Difference of air temperature and temperature average of height (Shading at 1 degC intervals) each observation point on Bussol Sea.

Figure 8 Difference of air temperature and temperature average of height based on IPRC Regional Climate Model CTL (top) and SST decrease run (bottom) (Shading at 1 degC intervals) each observation point on Bussol Sea.

Figure 9 Difference of CTL and SST decrease run air temperature average of SST decrease area (shading 1 degC intervals) in July 1998.

Figure 10 (top) Difference of CTL and SST decrease run heat budget average of SST down area (shading 0.5 degC/day intervals) in July 1998. (bottom) In a similar way, vertical flow (shading 0.01 ω interval).

Figure 11 Sea surface pressure based on IPRC Regional Climate Model CTL (shading 2 hPa intervals), on 11 July 1998 (a), 12 July 1998 (b), 13 July 1998 (c), 14 July 1998 (d).

Figure 12 Sea surface pressure based on IPRC Regional Climate Model SST decrease run (shading 2 hPa intervals), on 11 July 1998 (a), 12 July 1998 (b), 13 July 1998 (c), 14 July 1998 (d).

Figure 13 Difference of CTL and SST decrease run average cloud cover between $\sigma = 0.982$ and $\sigma = 0.942$ based on IPRC Regional Climate Model SST decrease run (shading 0.1 cloud cover intervals), on 11 July 1998 (a), 12 July 1998 (b), 13 July 1998 (c), 14 July 1998 (d).

Figure 14 Difference of sea surface pressure based on IPRC Regional Climate Model CTL and SST decrease run (shading 2 hPa intervals), on 11 July 1998 (a), 12 July 1998 (b), 13 July 1998 (c), 14 July 1998 (d).

Figure 15 Difference of sea surface pressure of composit analysis based on IPRC Regional Climate Model CTL and SST decrease run (shading 0.1 hPa intervals). The condition of composit is that the area average pressure of $145^{\circ}\text{E} - 155^{\circ}\text{E}$, $48^{\circ}\text{N} - 54^{\circ}\text{N}$ is or more 6.5hPa than the area average pressure of the same longitude $36^{\circ}\text{N} - 42^{\circ}\text{N}$.

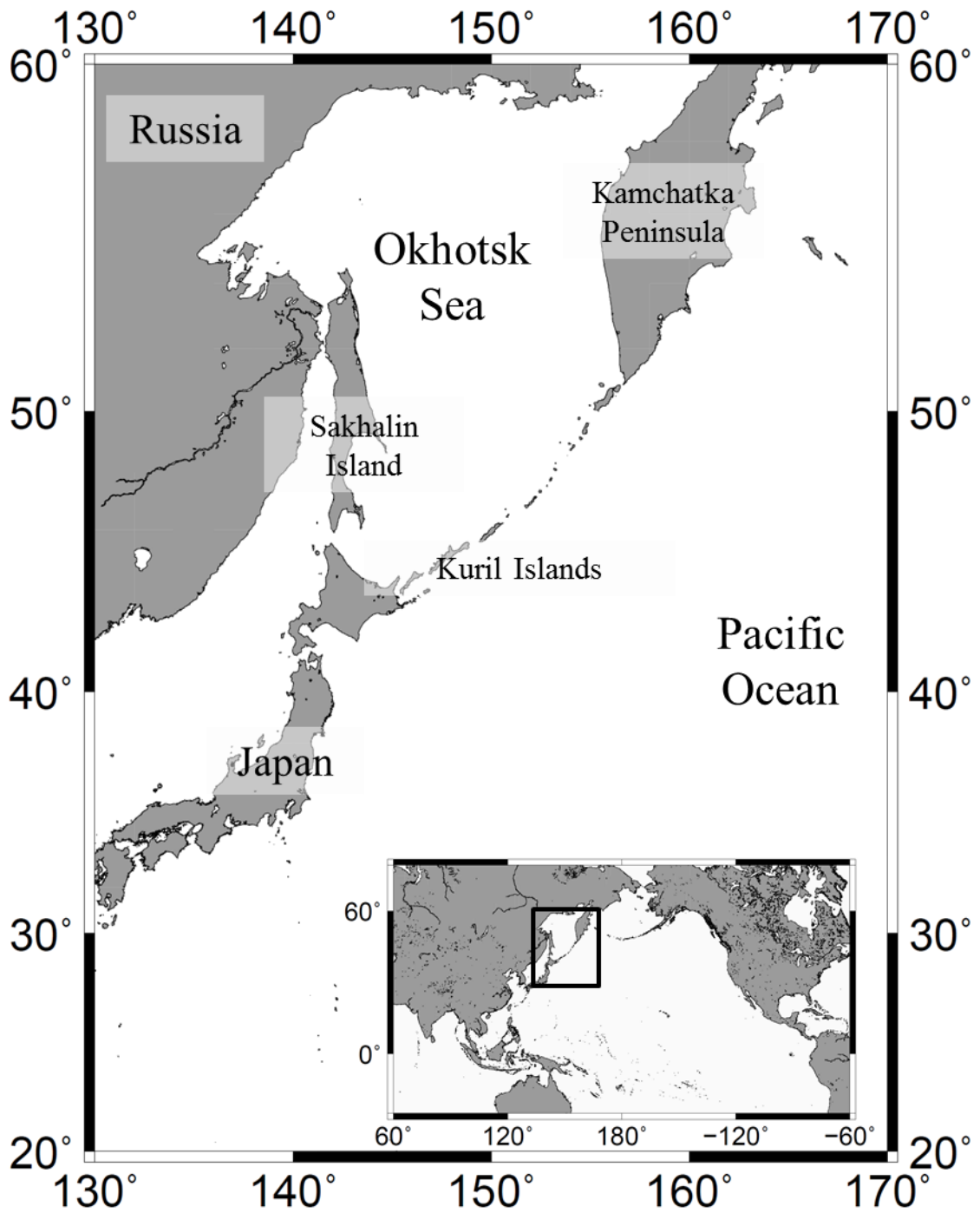


Figure 1 Map of the Okhotsk Sea and Kuril Islands.

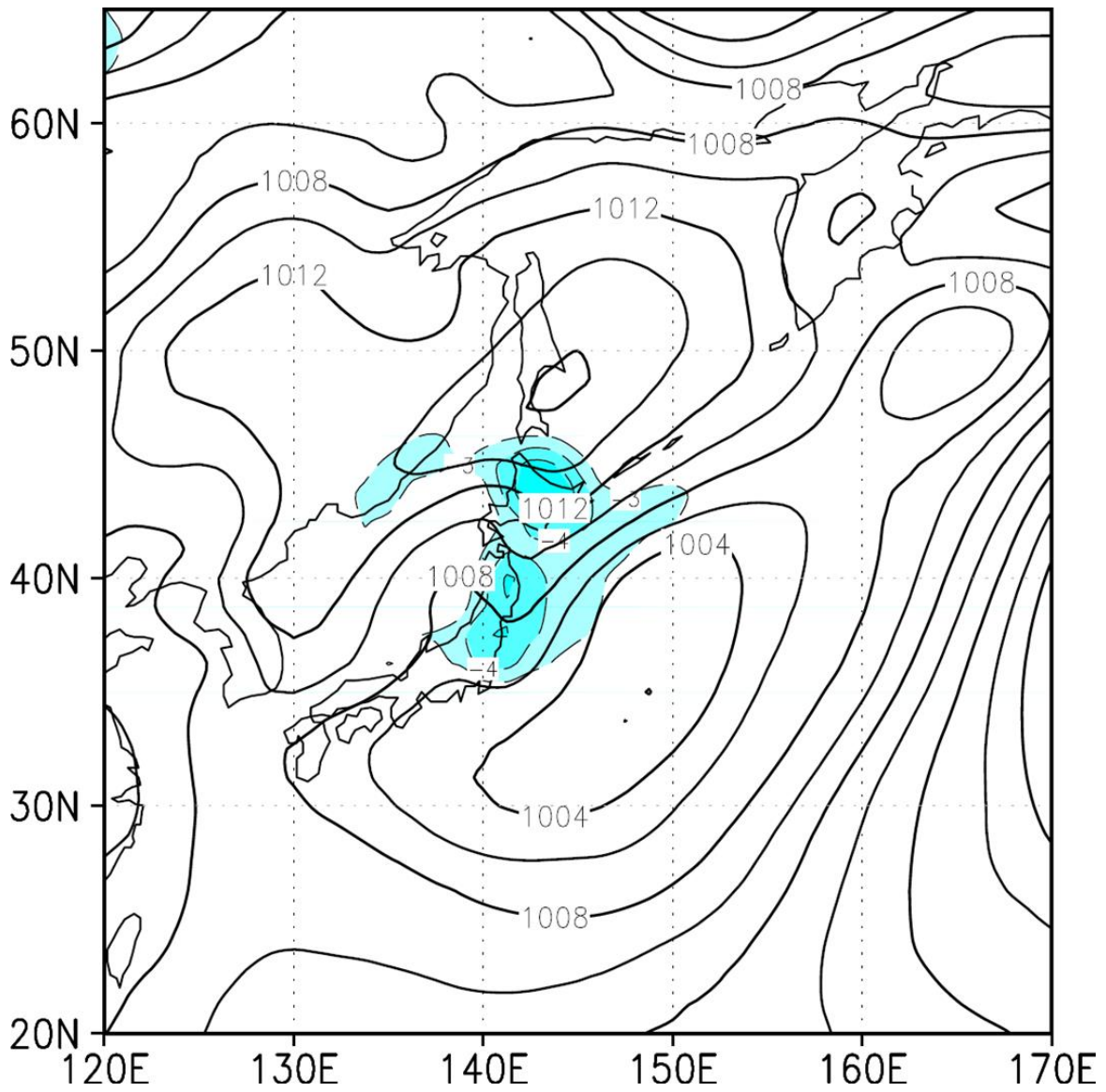


Figure 2 Surface weather chart based on the JRA25, showing unfiltered mean-sea-level pressure for 12 July 1998 (heavy solid lines at 2 hPa intervals), inferred surface air temperature anomalies (dashed lines and shaded at -3, -4, -5 degC).

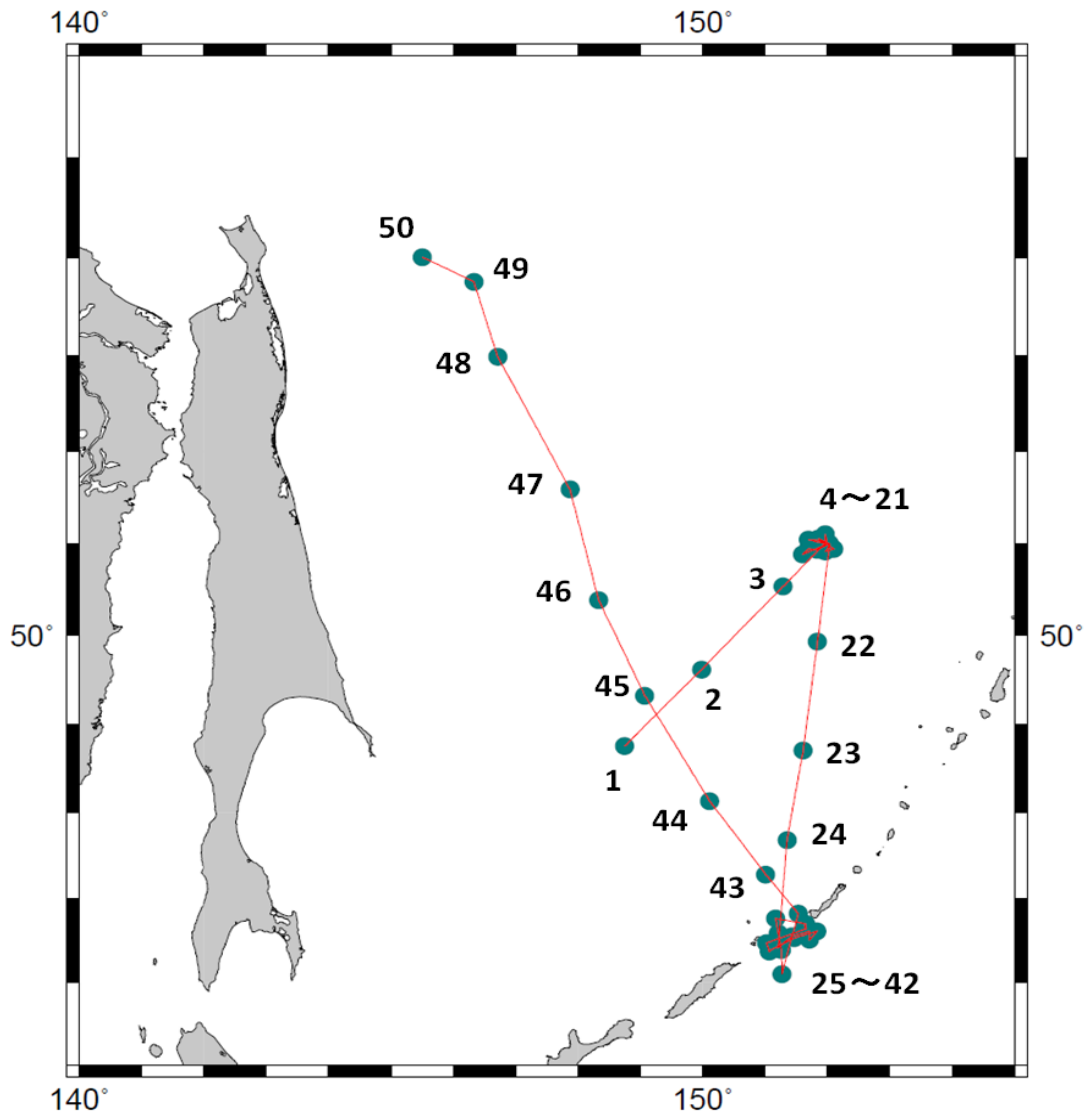


Figure 3 The observation route of Khromov in 1998, showing observation point (blue dot) and observation number.

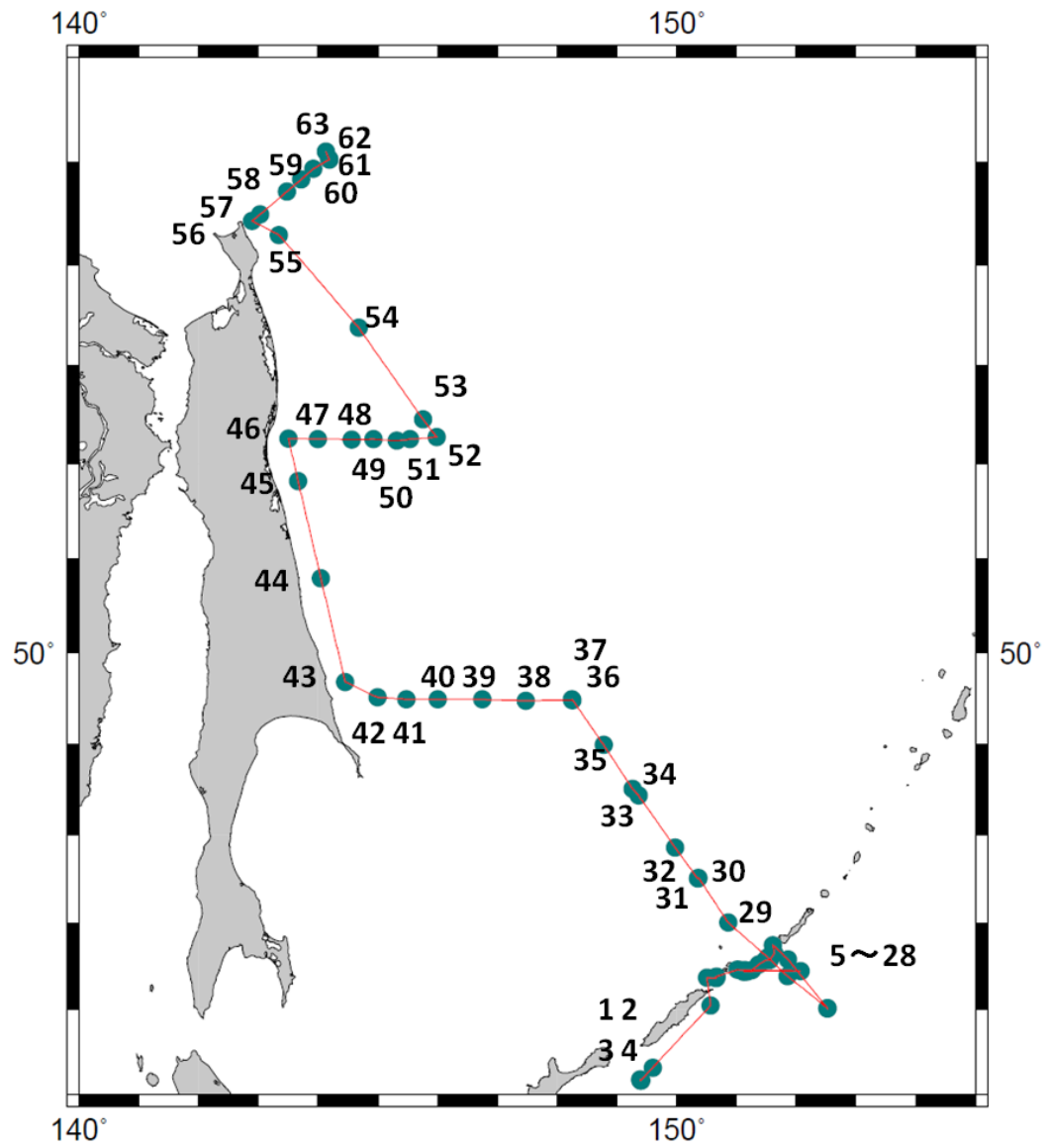


Figure 4 The observation route of Khromov in 2006, showing observation point (blue dot) and observation number.

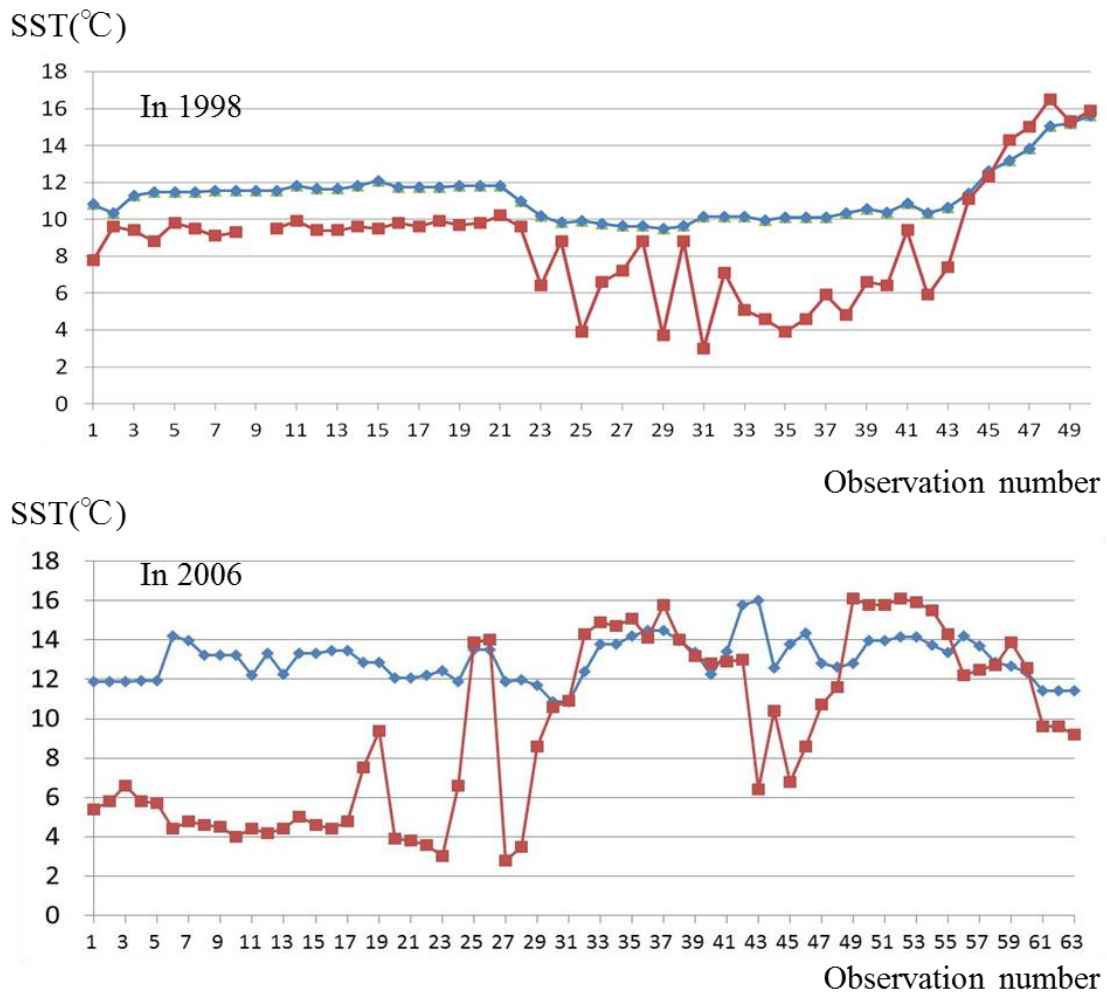


Figure 5 SST observed by Khromov (red line) and SST based on NOAA OISST of the nearest grid from observation point (blue line). Top is in 1998, and bottom is in 2006.

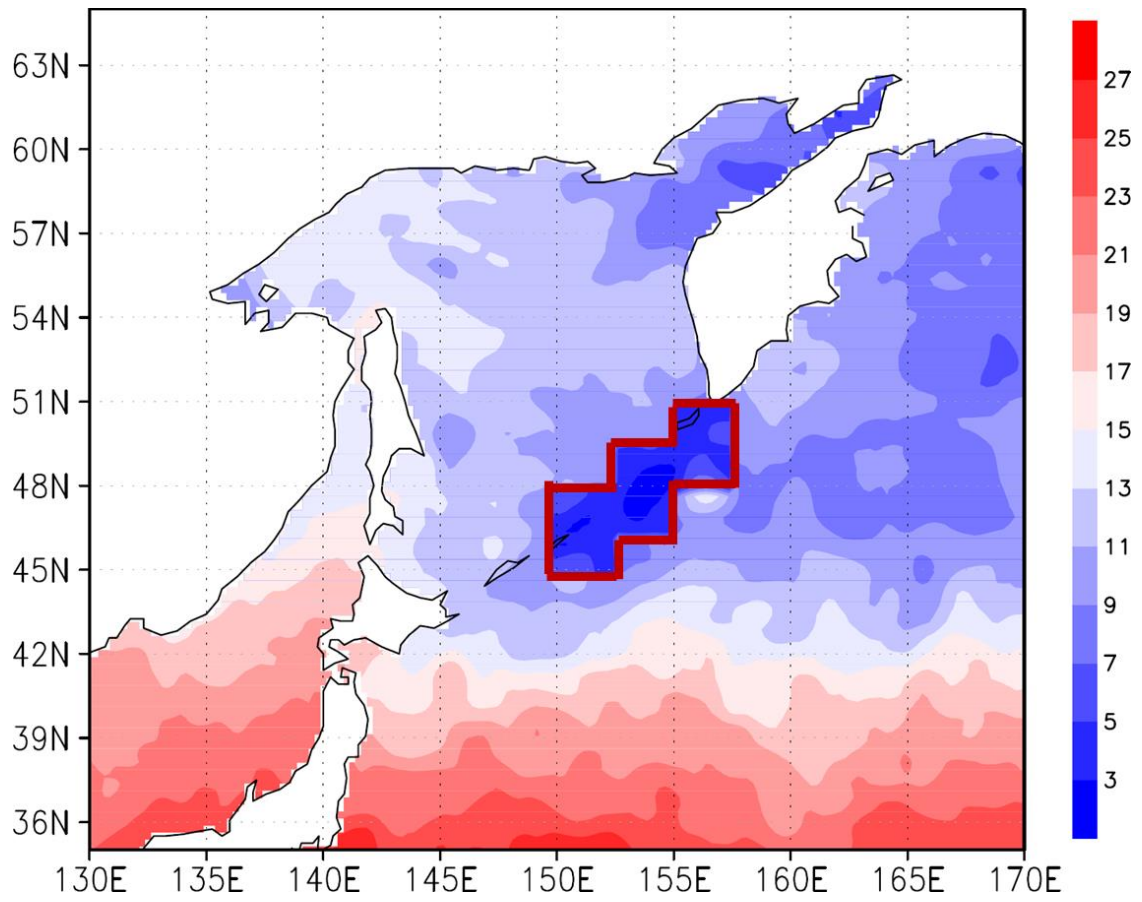


Figure 6 SST based on NOAA OISST (daily) (shading 2 degC intrvals) of SST decrease run in 17 July. Red frame area is SST decrease area.

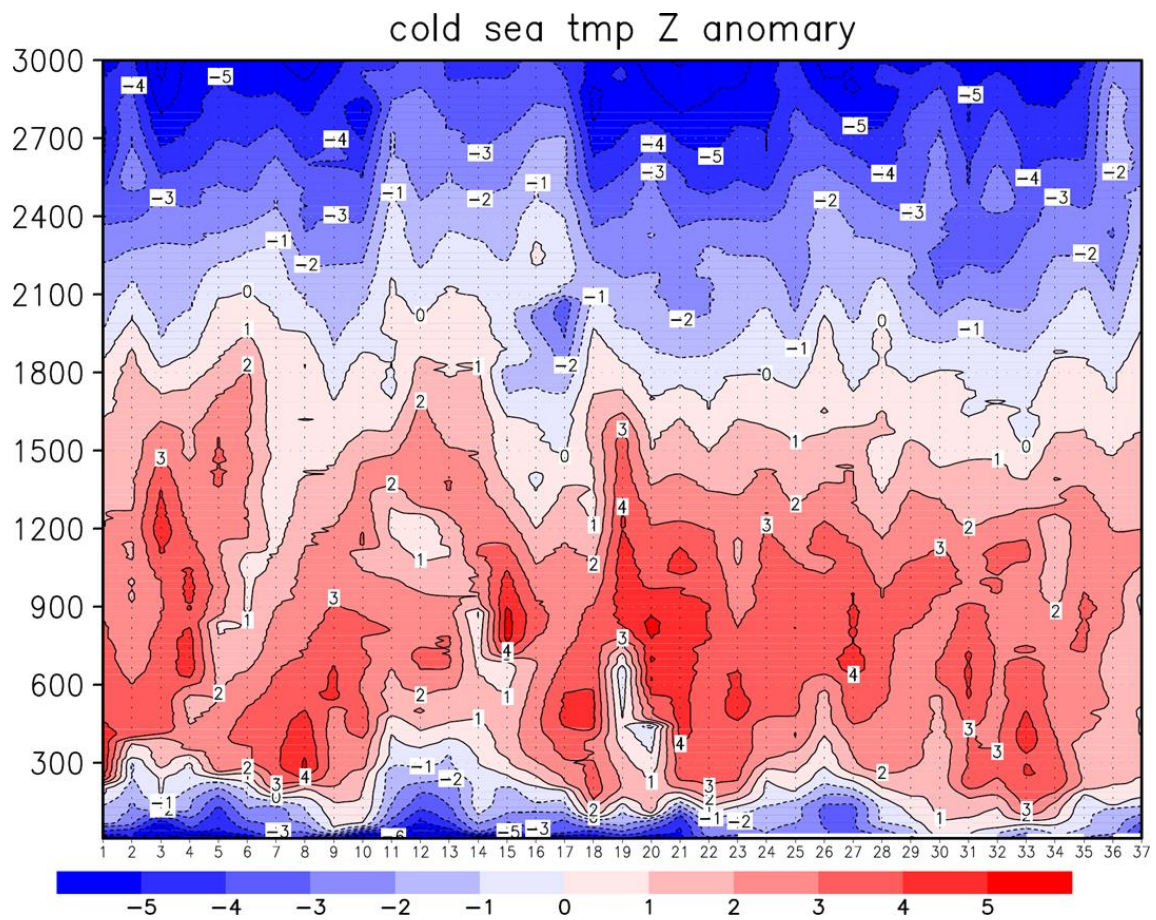


Figure 7 Difference of air temperature and temperature average of height (Shading at 1 digC intervals) each observation point on Bussol Sea.

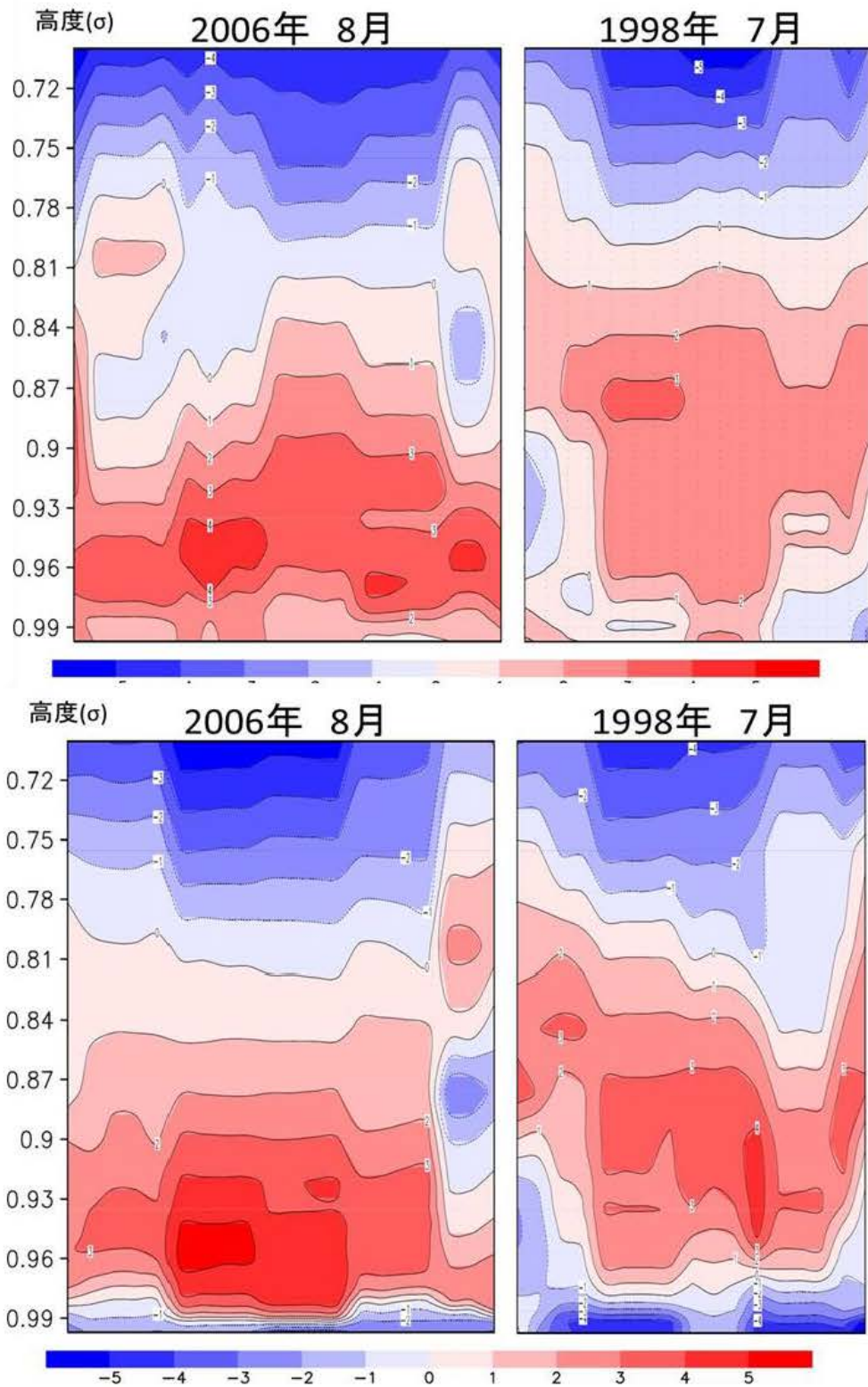


Figure 8 Difference of air temperature and temperature average of height based on IPRC Regional Climate Model CTL (top) and SST decrease run (bottom) (Shading at 1 digC intervals) each observation point on Bussol Sea.

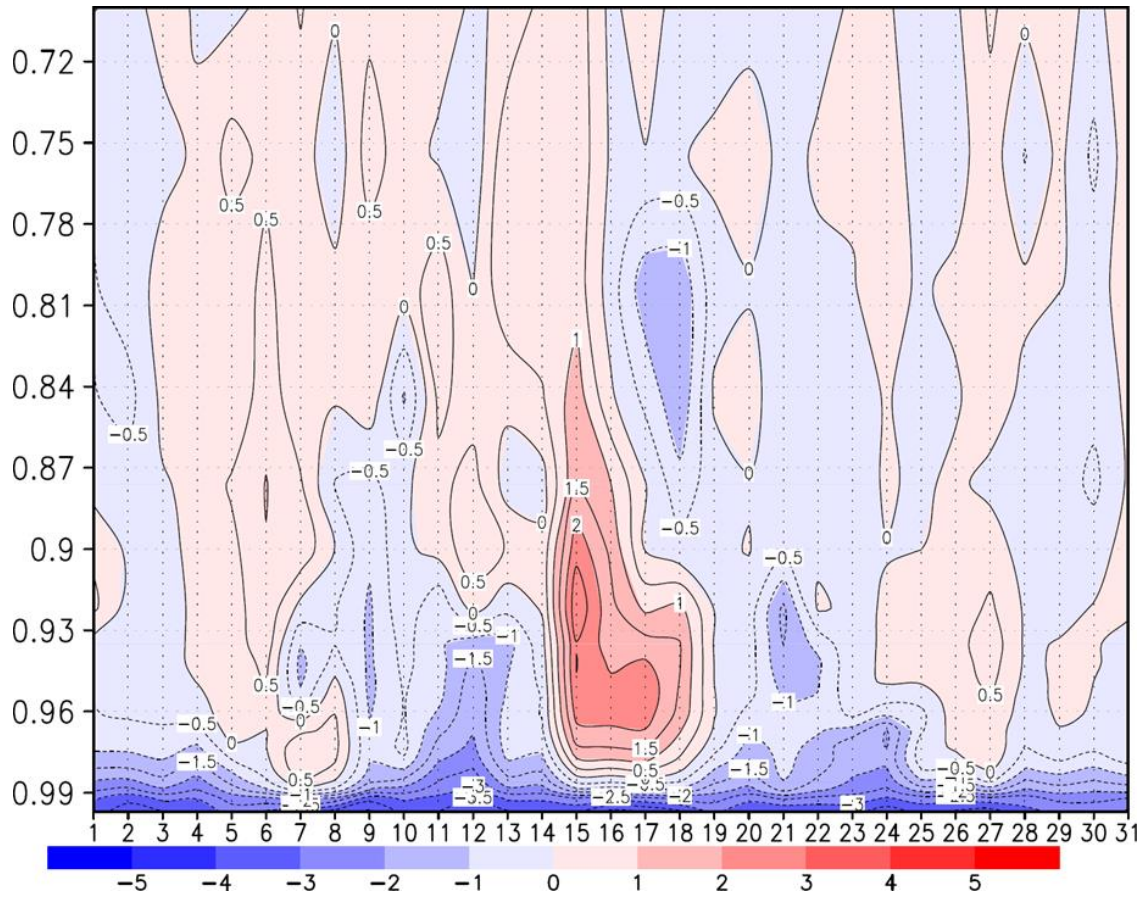


Figure 9 Difference of CTL and SST decrease run air temperature average of SST down area (shading 1 degC intervals) in July 1998.

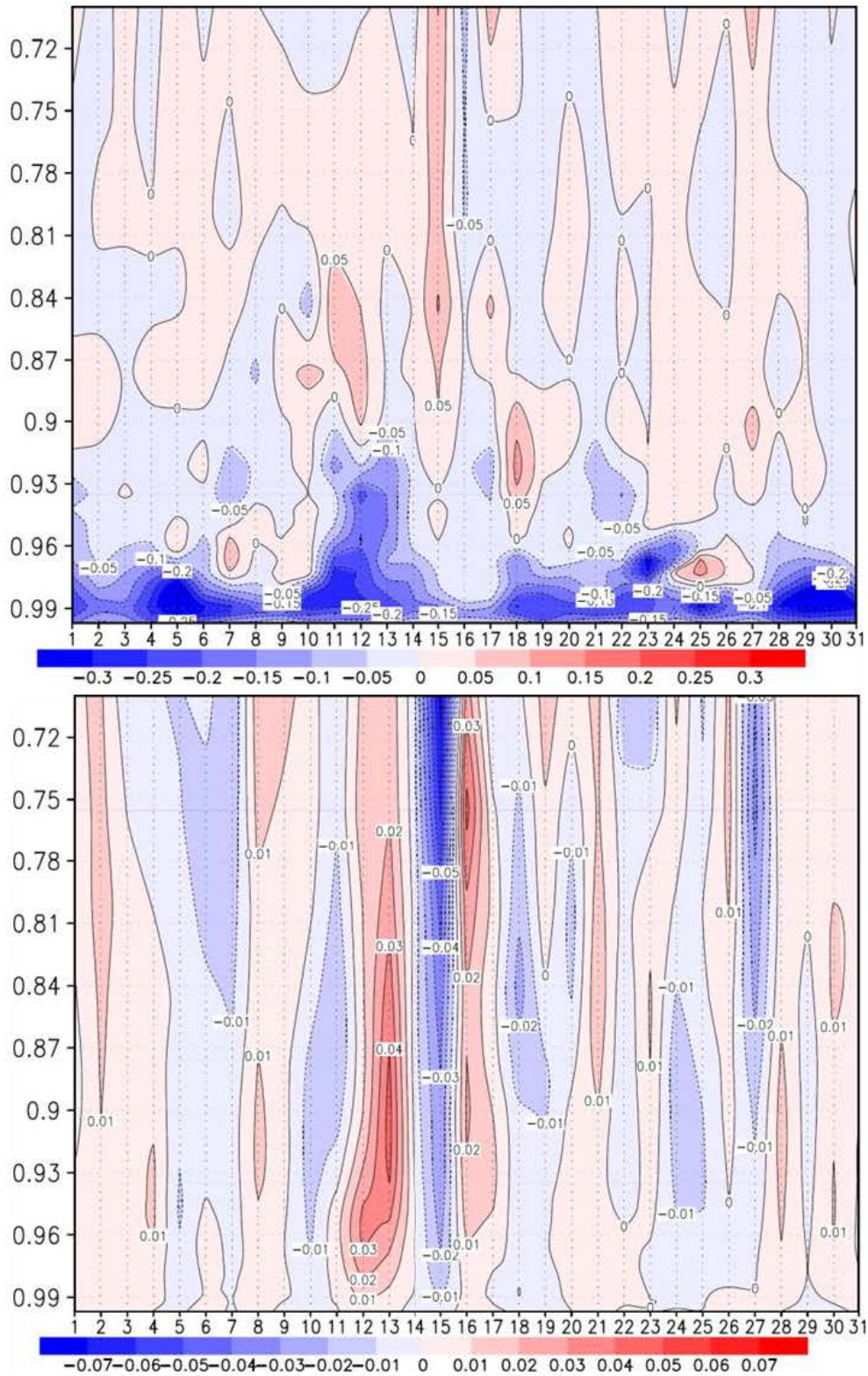


Figure 10 (top) Difference of CTL and SST decrease run heat budget average of SST down area (shading 0.5 degC/day intervals) in July 1998. (bottom) In a similar way, vertical flow (shading 0.01 ω intervals).

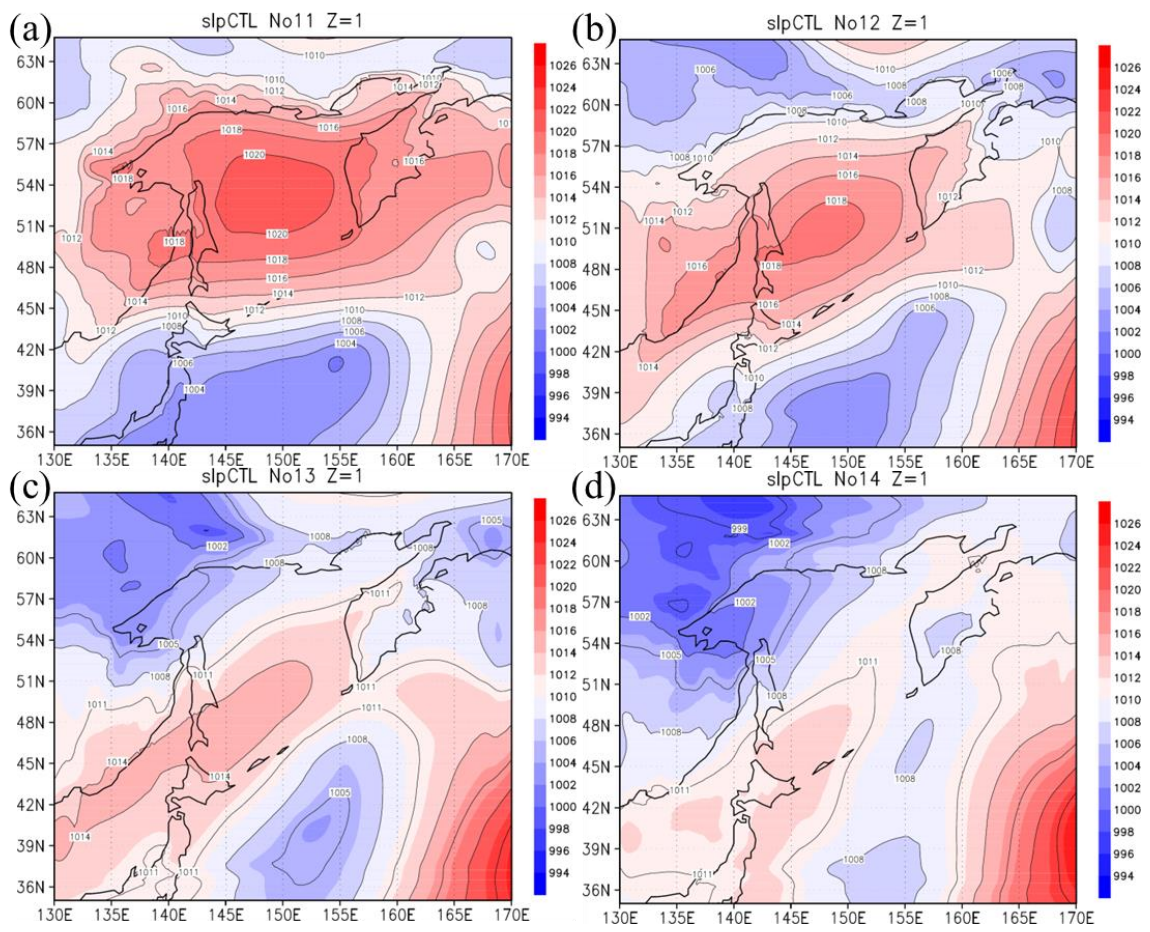


Figure 11 Sea surface pressure based on IPRC Regional Climate Model CTL (shading 2 hPa intervals), on 11 July 1998 (a), 12 July 1998 (b), 13 July 1998 (c), 14 July 1998 (d).

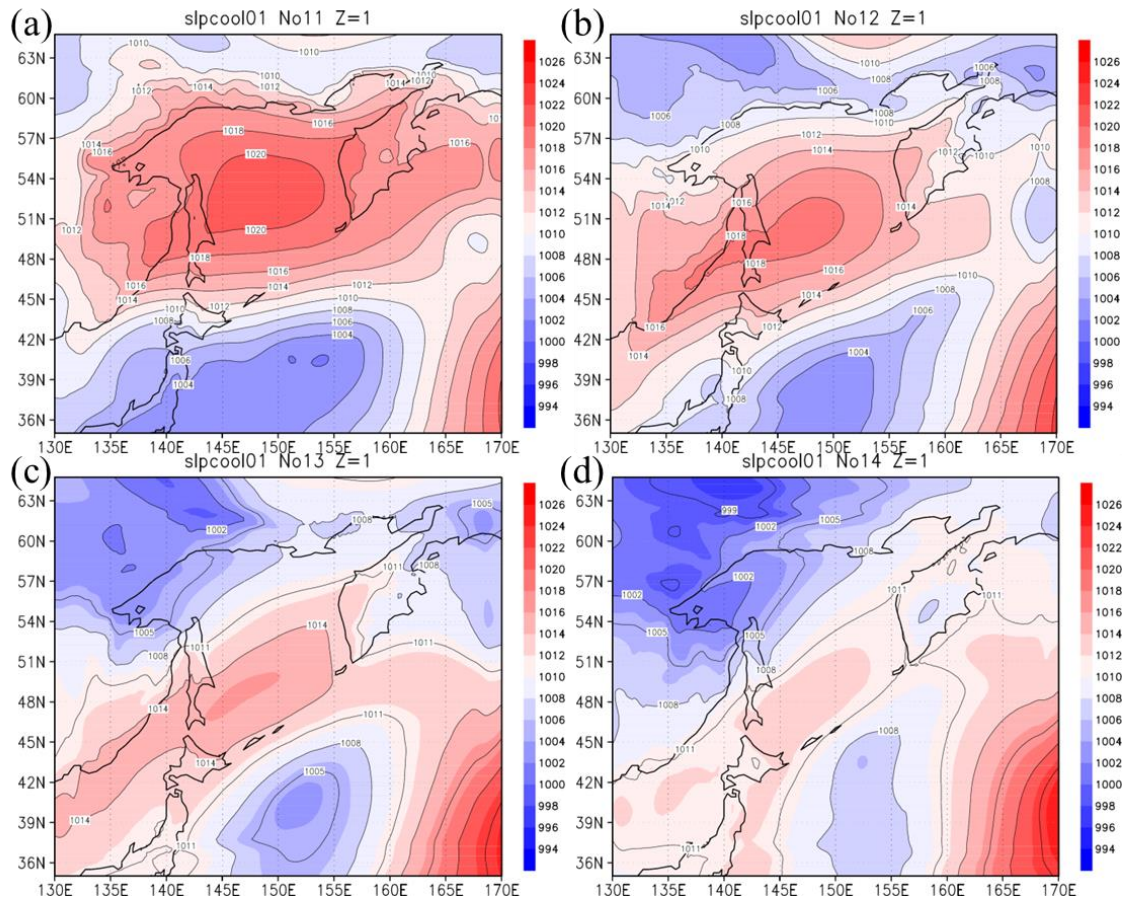


Figure 12 Sea surface pressure based on IPRC Regional Climate Model SST decrease run (shading 2 hPa intervals), on 11 July 1998 (a), 12 July 1998 (b), 13 July 1998 (c), 14 July 1998 (d).

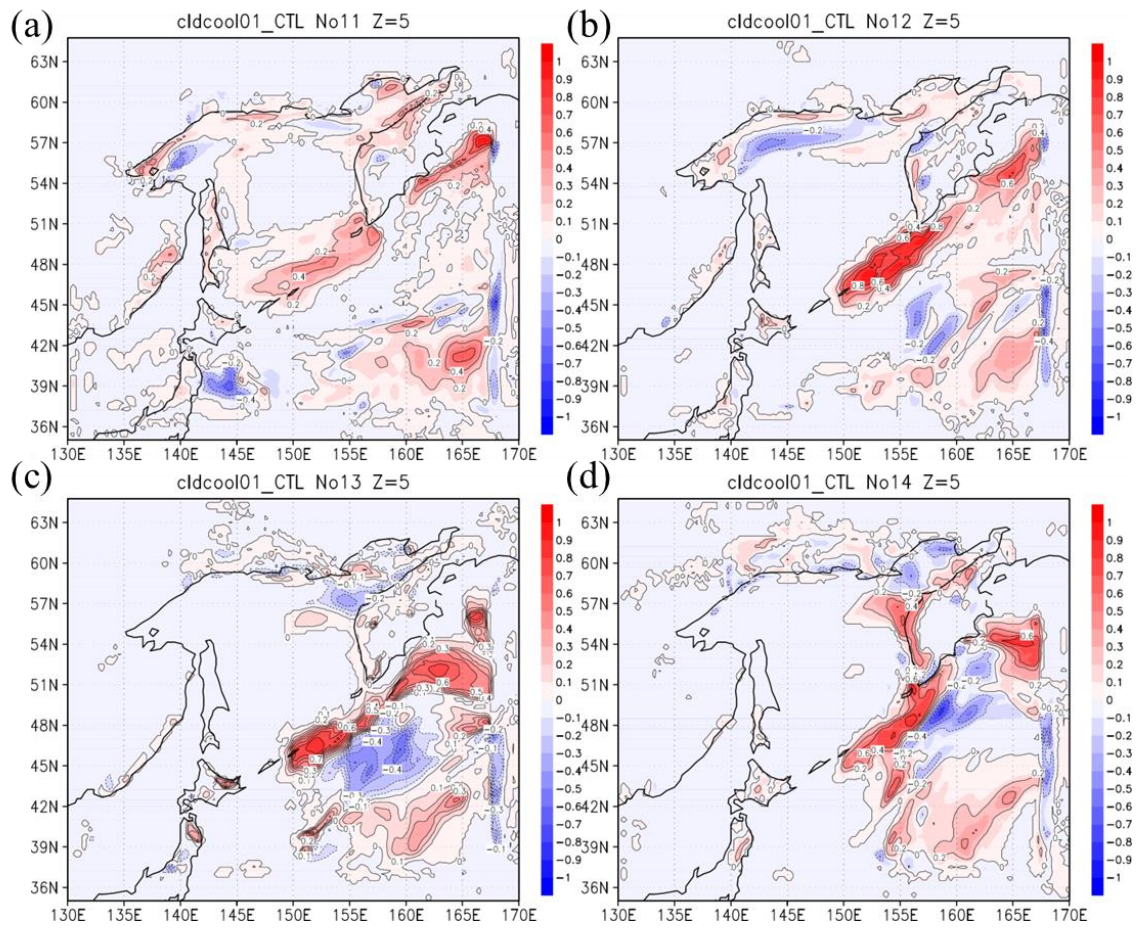


Figure 13 Difference of CTL and SST decrease run average cloud cover between $\sigma = 0.982$ and $\sigma = 0.942$ based on IPRC Regional Climate Model SST decrease run (shading 0.1 cloud cover intervals), on 11 July 1998 (a), 12 July 1998 (b), 13 July 1998 (c), 14 July 1998 (d).

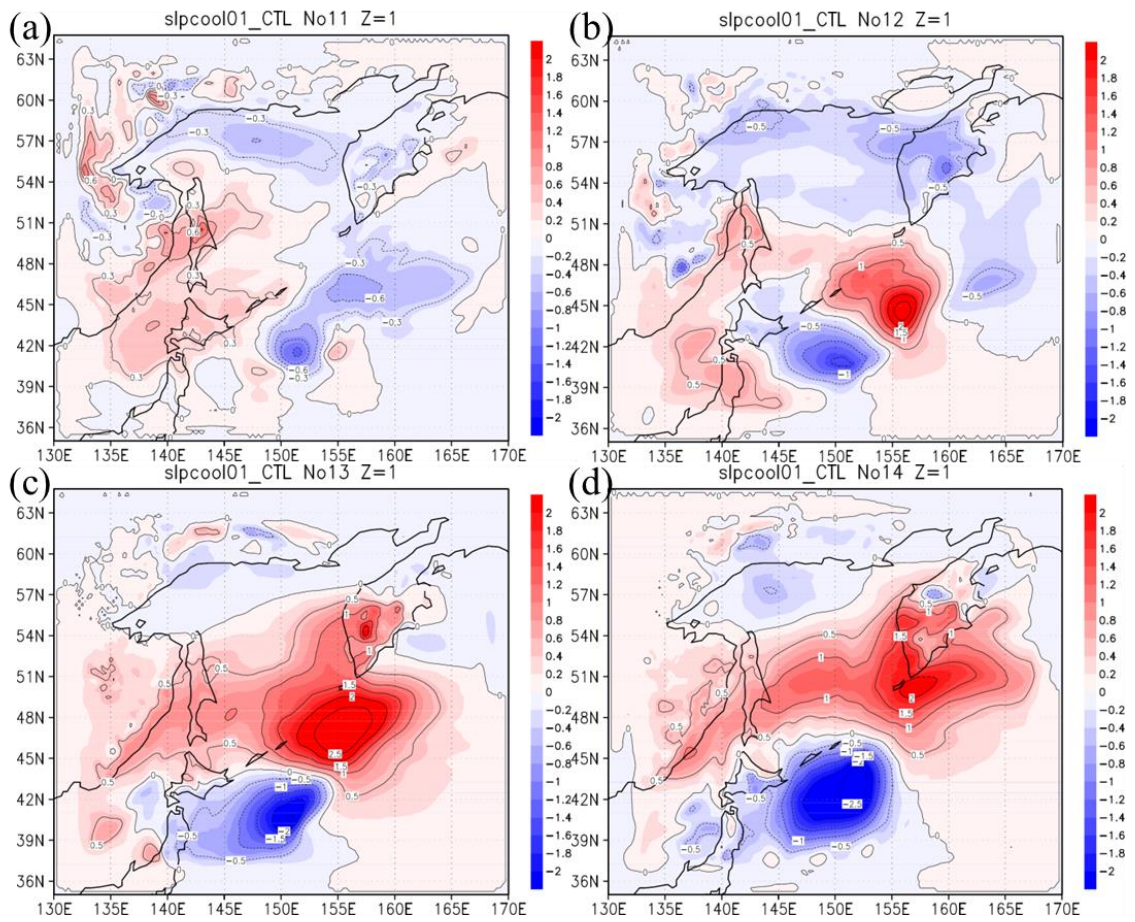


Figure 14 Difference of sea surface pressure based on IPRC Regional Climate Model CTL and SST decrease run (shading 2 hPa intervals), on 11 July 1998 (a), 12 July 1998 (b), 13 July 1998 (c), 14 July 1998 (d).

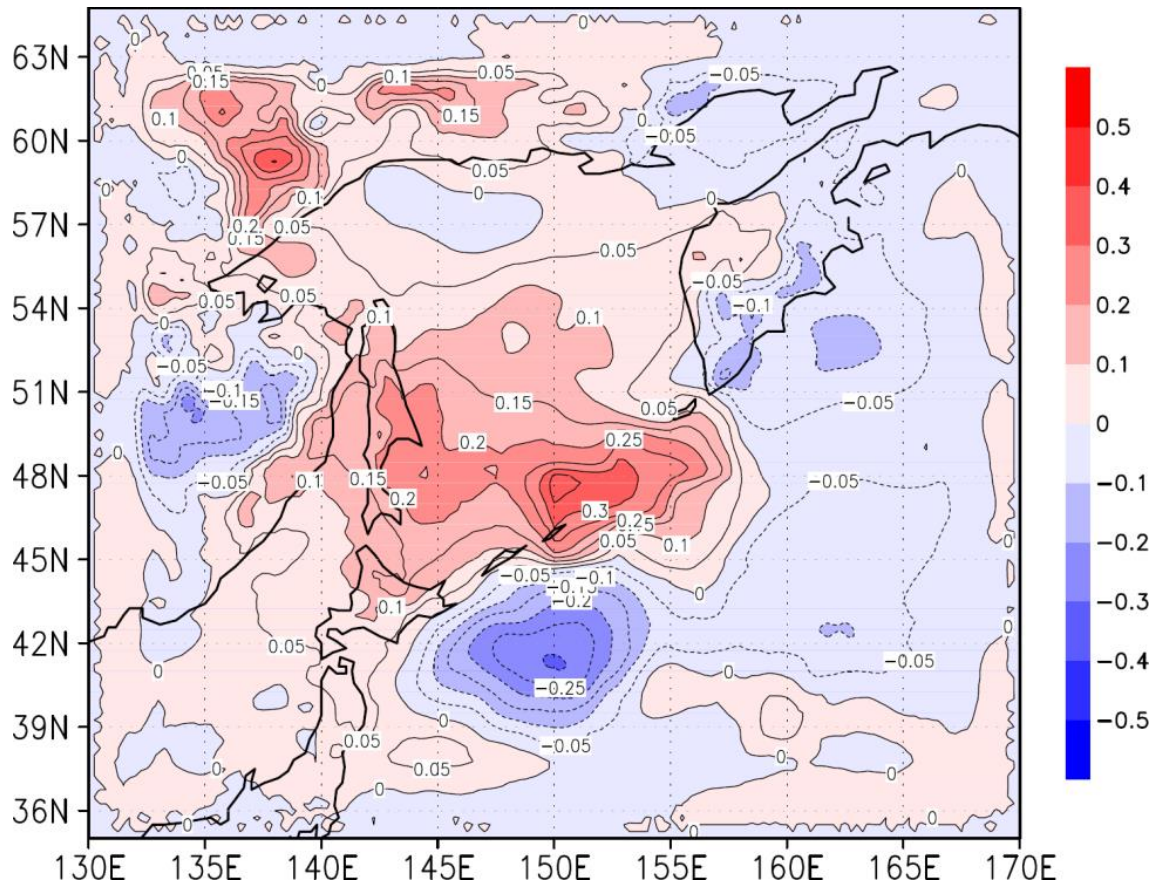


Figure 15 Difference of sea surface pressure of composite analysis based on IPRC Regional Climate Model CTL and SST decrease run (shading 0.1 hPa intervals). The condition of composite is that the area average pressure of 145°E – 155°E, 48°N – 54°N is or more 6.5hPa than the area average pressure of the same longitude 36°N – 42°N.